RSC Advances

PAPER

View Article Online
View Journal | View Issue

Cite this: *RSC Adv.*, 2016, **6**, 24889

Synthesis and ultrafast spectroscopic study of new [6,6]methanofullerenes†

Samya Naqvi,‡[a] Neha Gupta,‡[a] Neelam Kumari,‡[a] Mukesh Jewariya,[bc] Pramod Kumar,[d] Rachana Kumar‡*[a] and Suresh Chand[a]

Received 14th January 2016
Accepted 26th February 2016

DOI: 10.1039/c6ra01189f

www.rsc.org/advances

Ultrafast transient absorption and terahertz spectroscopic studies have been performed on new [6,6] methanofullerenes synthesized by the reaction of diazomethane (generated *in situ* from their hydrazone precursor) with fullerene[60] *via* our eco-friendly methodology, *i.e.*, amine-assisted 1,3 dipolar cycloaddition (AACA). Synthesized materials have been characterized by different spectroscopic techniques for their structure establishment, including terahertz spectroscopy to study changes in spectra on functionalization. Attachment of different types of functional groups on exohedral chains resulted in band gap tuning. Photoinduced charge generation and charge separation studies have been performed to understand the charge carrier dynamics in a methanofullerene : P3HT mixture. Efficient charge separation efficiency is observed in both the acceptors on mixing with P3HT, making them potential acceptor materials in organic solar cells. High photoconductivity calculated by terahertz time domain spectroscopy of these new fullerene derivatives can also be exploited in other organic electronic devices.

1. Introduction

Fullerene[60] derivatives *via* exohedral functionalization offer potential applications in diverse areas.[1–6] The development of different methods for the functionalization of the fullerene molecule is of great significance as it opens up new routes for the functionalization of other carbon materials. For the functionalization of this magical ball, commonly used strategies are [2 + 1], [2 + 2], [3 + 2], and [4 + 2] cycloadditions, nucleophilic addition reactions and radical reactions.[7–12] Among all the reactions, cyclopropanation by 1,3 dipolar or carbene addition reactions have been exploited extensively for synthesis of various fullerene derivatives for solar cells applications.[13–16] Phenyl[C61]butyric acid methyl ester (PC61BM) is one of the example synthesized by 1,3 dipolar cycloaddition of diazo compound and being extensively used in organic photovoltaics (OPV) with various donor materials.[17–19] Several fullerene derivatives have been synthesized to improve power conversion efficiency (PCE) by improving the open circuit voltage (V_{oc}) as the V_{oc} of a bulk-heterojunction photovoltaic cell scales linearly with the decrease of the first reduction potential of the acceptor.[20]

We have recently reported a cost effective and eco-friendly method of 1,3 dipolar cycloaddition reaction for the synthesis of most conventional electron acceptor material [6,6]PC61BM in bulk heterojunction organic solar cells by *in situ* generation and cycloaddition of diazo compound in presence of mild base (amine assisted 1,3 dipolar cycloaddition (AACA)) in good yield and purity under aerobic condition.[16] Several other methods are also reported for catalytic cycloaddition reaction of *in situ* generated diazo compounds on fullerene.[21,24] In the present study we have synthesized new methanofullerene derivatives having different substituents on exohedral chain for tuning of energy levels. The synthesized products have been characterized by FTIR, UV-vis, NMR and terahertz spectroscopy for their structure[22] and analyzed by cyclic voltammetry for their electrochemical behaviour and calculation of highest occupied molecular orbitals (HOMO)–lowest unoccupied molecular orbitals (LUMO) levels. For their future application as acceptors in organic solar cells it is very essential to study the photophysics and decay dynamics of charge transfer states generated on mixing with donor polymer. There are several limiting factors for solar cells performance and charge recombinations are one of them.[23] Transient absorption spectroscopy is an important tool to study the formation of transient species whether emissive or non-emissive on excitation with pump

[a]*CSIR-National Institute of Solar Energy, Organic and Hybrid Solar Cells Group, Physics of Energy Harvesting Division, CSIR-National Physical Laboratory, New Delhi-110012, India. E-mail: rachanak@nplindia.org; Fax: +91-11-4560-9310; Tel: +91-11-4560-8620*

[b]*Ultrafast Optoelectronics and Terahertz Photonics Lab, Physics of Energy Harvesting Division, CSIR-National Physical Laboratory, New Delhi 110012, India*

[c]*Center for Quantum-Beam-based Radiation Research, Korea Atomic Energy Research Institute (KAERI), Korea*

[d]*Magnetic and Spintronic Laboratory, Indian Institute of Information Technology Allahabad, Allahabad 211012, India. E-mail: pkumar@iiita.ac.in*

† Electronic supplementary information (ESI) available. See DOI: 10.1039/c6ra01189f

‡ Academy of Scientific and Innovative Research, New Delhi.

wavelength.[24,25] Here we have performed a detailed discussion on generation and decay dynamics of charge transfer states in methanofullerene : P3HT mixtures and compared with PC61BM : P3HT mixture. Fluorescence decay kinetics has also been performed in blend solution by transient fluorescence spectroscopy. Photoconductivity has been calculated from terahertz time domain spectroscopy data for both the products and compared with parent fullerene[60].

2. Results and discussion

In order to modify the intrinsic electron-acceptor property of pristine fullerene[60] for the optimized redox behaviour to be exploited in OPV, a great number of reactions are reported for its chemical modification along with modification in electronic properties. Very recently Martin and co-workers have reported the synthesis and characterization of dumbbell molecules where two fullerene molecules are connected to a central fluorene bridge *via* two different types of connections, *i.e.*, (i) substituted pyrrolidine (Py) and (ii) cyclopropane (Cp) group and calculated theoretically and experimentally the enhanced electronic communication through the cyclopropane group compared to pyrrolidine analogue which works as quasi-double bond.[26] Keeping this in mind we have synthesized new methanofullerene molecules (Fig. 1) where a double bond is working as a bridge to connect the cyclopropane ring on fullerene to the terminal moiety containing different functional groups. Product **1** contains phenyl ring pendant on the cyclopropane ring while in product **2** it is only a proton. Kim *et al.*, have demonstrated the sensitivity of the LUMO energy level of the fullerene derivatives to the nature of addends with the carbazole functionalized fullerene where the reduction value of Py connected compounds showed huge anodic shift and in contrast to Cp connected compounds which show cathodic shift raising the LUMO energy.[27] So far the best approach for the cyclopropanation addition to fullerene[60] is through the 1,3 dipolar cycloaddition of diazo compound generated from their tosylhydrazone precursors in pyridine in presence of sodium methoxide under inert atmosphere.[14] In the present work, we have followed our more promising AACA approach for the cyclopropanation reaction which is more eco-friendly and occurs under aerobic conditions with excellent yield and purity.[16]

Fig. 2A presents the general methodology for the synthesis of enone (chalcone) *via* Claisen–Schmidt condensation of acetophenone with the respective aldehyde and preparation of

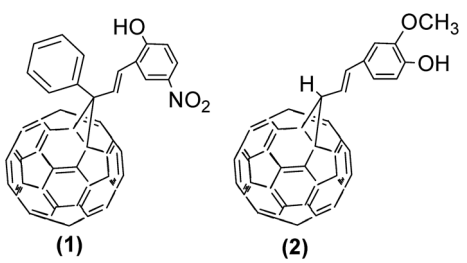

Fig. 1 Structure of synthesized methanofullerene **1** & **2**.

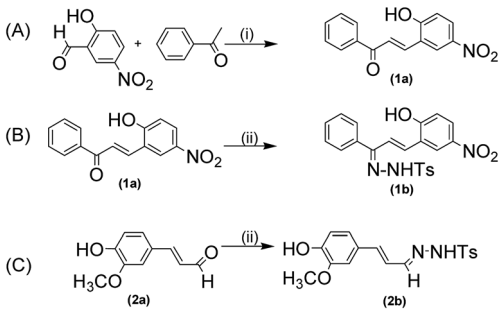

Fig. 2 Synthesis of (A) chalcone (**1a**) (i) ethanol, 40% NaOH solution, r.t.; (B–D) synthesis of tosylhydrazone (**1b**, **2b**) of **1a**, **2a** (ii) *p*-tosyl sulfonyl hydrazide, methanol, reflux, 6 hours.

hydrazones from their respective chalcones or cinnamaldehydes in methanol. The reaction of 2-hydroxy-5-nitro benzaldehyde with acetophenone converts it into enone **1a** where, α, β double bond is present to phenyl ketone (A). These chalcones have several biological applications, however, we have exploited their use in fullerene chemistry. Cinnamaldehyde compound **2a** is available commercially.

Enone **1a** & **2a** were converted into their respective tosylhydrazones (**1b**, **2b**) (Fig. 2B and C) by reaction with *p*-toluene sulfonyl hydrazide. Tosylhydrazones are the best precursors for the synthesis of diazo compound for cyclopropanation reaction with fullerene. Earlier it was suggested that all diazomethane addition forms π-homoaromatic [6,6] open structures but revised later to α-homoaromatic [6,6] closed methanofullerene structures.[15] Several types of catalytic diazo generation and decomposition reactions are reported, among which are thermal reactions of diazo compounds with fullerene[60], metal catalyzed reactions, photolysis of diazo compounds, *in situ* generation by thermolysis *etc.* Treatment of tosylhydrazones with metal alkoxide generates diazo compounds *in situ* under controlled environment. In our AACA approach we have generated diazomethane intermediate *in situ* in presence of tert. amine under aerobic condition. For the reaction of **1b** with fullerene[60], first diazo was prepared *in situ* in dichloromethane at 0 °C, using triethyl amine as catalyst. *o*-Dichlorobenzene solution of C_{60} is added and heated at 80 °C for 18 hours. Reaction mixture was concentrated and subjected to column chromatography to collect the second band after unreacted fullerene giving single spot in TLC. This is the kinetically favourable [5,6]fulleroid (in ^{13}C NMR bridgehead carbon appears at 64 ppm). Refluxing this fulleroid in *o*-dichlorobenzene converts totally to methanofullerene **1** by thermal isomerisation (Fig. 3).

The structure of the fullerene adduct **1** has been confirmed by spectroscopic techniques. FTIR clearly shows the presence of C=C double bond (1634 cm^{-1}), –OH group (3458 cm^{-1}) and NO_2 group (1511 cm^{-1}). ^{1}H NMR and ^{13}C NMR further confirm the formation and purity of [6,6]methanofullerene (1) where the bridging carbon and bridgehead carbons appear at 64 and 89 ppm respectively in ^{13}C NMR. Vogel and co-workers[28] have explored in the study of π *vs.* σ homoaromaticity for methanoannulenes through ^{13}C NMR chemical shifts that the

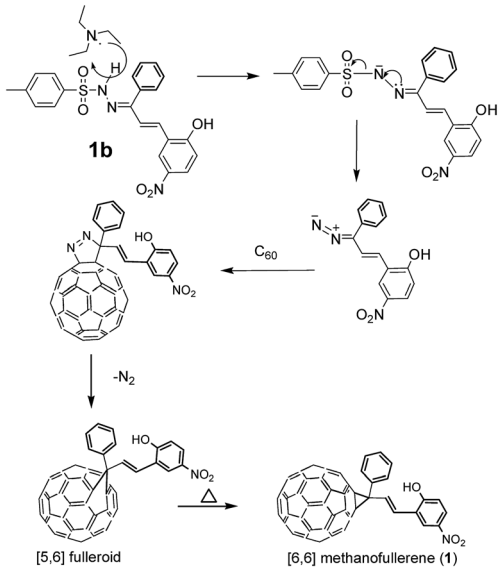

Fig. 3 Synthesis and mechanism of product **1** formation from hydrazone **1b**.

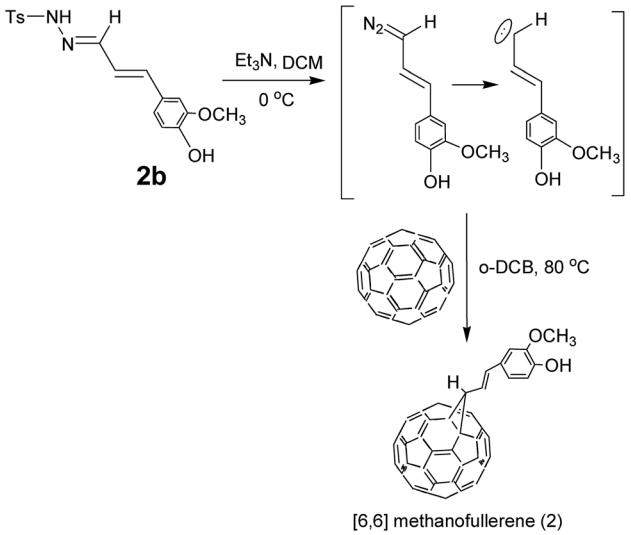

Fig. 4 Synthesis and mechanism of product **2** formation from hydrazone **2b**.

resonance of bridgehead carbon atom for closed σ homoaromatic structure appear at high field (40–60 ppm) whereas, for open π homoaromatics it shifts to downfield into aromatic olefinic region (*ca.* 110–120 ppm).

Similar to above, tosylhydrazones **2b** was prepared by refluxing **2a** with *p*-toluene sulfonyl hydrazide in methanol. On cooling down the reaction mixture, the crystals of hydrazone separate out and washed with cooled methanol, dried and used for next step reaction with fullerene[60]. Similar to phenyldiazoenone reaction, aerobic reaction conditions were used for reaction in presence of triethyl amine base in cooled dichloromethane. After 3 hours, *o*-dichlorobenzene solution of fullerene[60] was added and temperature was raised to 80 °C. The progress of the reaction was monitored by TLC. The reaction completes faster compared to (1). Reaction mixture was evaporated in rota-vapor and put on silica gel column for purification. Product **2** was collected after small amount of unreacted fullerene using toluene as eluent. NMR data completely supports the formation and high purity of monoadduct with [6,6]methanofullerene geometry. Direct synthesis of [6,6] adduct suggests that the reaction proceeds through carbene intermediate formation. A proposed mechanism for product **2** formation is given in Fig. 4. As an evidence for the [6,6]methanofullerene addition, ^{1}H NMR spectrum of **2** shows the typical chemical shift at 4.8 ppm for the C(61) proton.[34] Similarly, the ^{13}C NMR chemical shift of the bridging and bridgehead carbons appeared at 67.7 and 86.0, 86.2 ppm respectively, being indicative of 58π electronic structure of fullerene and formation of methanofullerene. A similar observation was reported by Diederich *et al.*, for the reaction of diazoacetate with fullerene[60] at room temperature for several days and later on in refluxing toluene. They suggested both, the formation of pyrazoline intermediate followed by rapid loss of N_2 molecules as well as thermal decomposition of diazocompound followed by addition of generated carbene for the formation of [5,6]fulleroid and [6,6]methanofullerene mixtures. Later on, Wang *et al.*, identified this reaction to proceed *via* carbene mechanism.[29,30]

Fig. 5 shows the absorption spectra of products (**1** & **2**) and compared with fullerene[60] parent molecule and PC61BM in chloroform solution (25 μM). On functionalization, the absorption bands of parent fullerene at 382 nm completely disappears with appearance of clear peaks at 435 and 697 nm for product **1** and at 435 and 707 nm for product **2** confirming the [6,6] addition on fullerene core akin to [6,6]PC61BM.[14] Product **2** shows extended absorption than 1 and band gap from absorption onset has been calculated to be 1.73 and 1.68 eV for product **1** & **2** respectively.

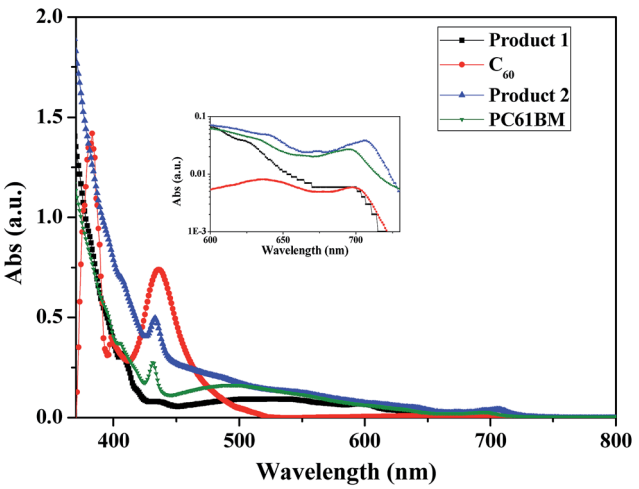

Fig. 5 Comparative UV-vis absorption spectra of products **1**, **2**, C_{60} and PC61BM in chloroform solution. Both the products show clear absorption band for [6,6]methanofullerene formation at ~700 nm and product **2** clearly shows extended absorption compared to **1** in inset.

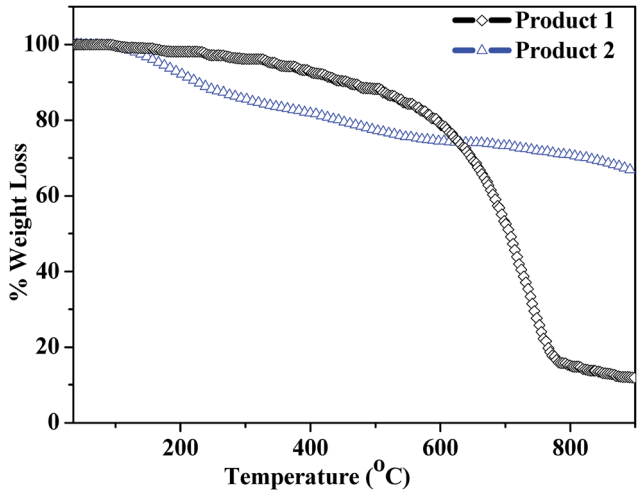

Fig. 6 TGA of products 1 & 2 under N_2 flow of 20 mL min^{-1} at 10 °C min^{-1} temperature ramping.

Thermal stability of the adducts has been compared by TGA analysis (Fig. 6). Both the products show good thermal stability up to 150 °C. Product **1** shows only 5% weight loss up to 400 °C. On the other hand product **2** shows continuous weight loss but least total decomposition of only 35% up to 900 °C compared to 86% for product **1**.

Electrochemical properties of the products were investigated by cyclic-voltammetry (CV) to determine the oxidation–reduction potentials and HOMO–LUMO levels as shown in Fig. 7. CV was performed in dry *o*-dichlorobenzene using 0.1 M supporting electrolyte (*n*-$TBAPF_6$). Three electrode system where, a platinum disc was used as working electrode, silver-wire and a platinum-wire as reference and counter electrode respectively. Ferrocene/ferricenium couple was an internal reference to calibrate the redox potentials. Both the products show two reversible reductions with half-cell potentials ($E_1 = 0.5[E_{p,c} + E_{p,a}]$) at −1.27, −1.80 V (product **1**) and at −1.27, −1.85 V (product **2**) for fullerene one and two electron reduction respectively.[14] LUMO energy level (Fig. 7) have been calculated from the onset reduction potential and was found to be ~−3.6 eV for both the products similar to PC61BM.[14,31,32] Product **2** shows lower oxidation onset compared to product **1** (1.08 *vs.* 1.13 V) and therefore lower band gap as seen in absorption spectra.

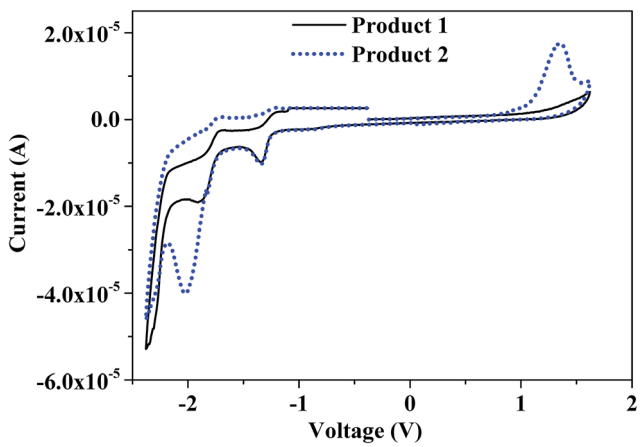

Fig. 7 Cyclic voltammogram of product **1** & **2** performed with a scan rate of 100 mV s^{-1} in 1 mM 0-dichlorobenzene solution using 0.1 M solution of $TBAPF_6$ as supporting electrolyte.

Both the products and their mixture with polymer (P3HT) in equimolar ratio in chloroform solution were also characterized by photoluminescence (PL) measurements. In both the cases strong PL quenching of 584 nm emission peak was observed (Fig. 8A) on excitation with 530 nm wavelength.[33] Quenching efficiency was compared using the formula,

$$\phi_q = (I_o - I)/I_o$$

where, I_o is the PL intensity of pure P3HT with same concentration and I is the PL intensity of P3HT : methanofullerenemixture. High quenching efficiencies obtained with the products indicate occurrence of better electron transfer interactions between donor (polymer) and acceptors. Products **1** & **2** show 77 and 98% quenching efficiency respectively. The optical

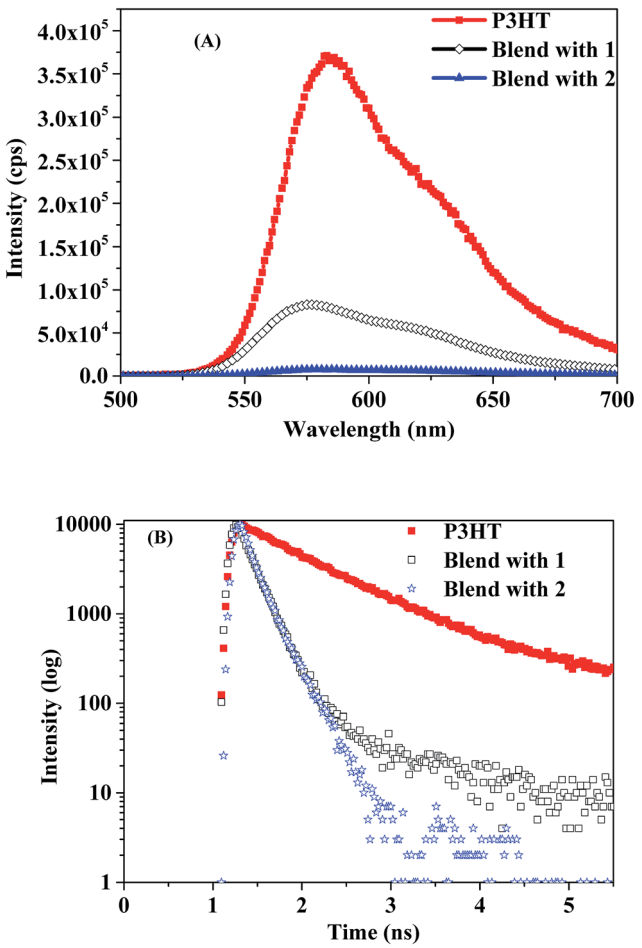

Fig. 8 (A) Fluorescence spectra of P3HT and its equimolar mixture with products **1** & **2** in chloroform to study the fluorescence quenching (λ_{ex} = 530 nm); (B) time correlated single photon spectroscopy was performed at 584 nm to study the decay kinetics of singlet excited state of P3HT in neat and on mixing with products **1** & **2**.

properties ascertain their promising candidature as acceptor material in organic photovoltaics.

Time correlated single photon counting (TCSPC) was performed to calculate the life time of singlet excited state of P3HT in neat and on mixing with products **1** & **2** (Fig. 8B). In the present work, photo-induced process have been studied in homogeneous solution to rule out the relatively fast charge recombinations in films due to improper morphology and traps formation. P3HT emission at 584 nm, due to singlet excited state relaxation, shows monoexponential decay kinetics with a lifetime (τ) of 0.85 ns *via* exciton–exciton annihilation.[34,35] While in mixtures the decay time is further reduced to 0.18 and 0.16 ns with product **1** & **2** respectively which is lower than P3HT : PCBM mixtures.[34] This further directly evidence for efficient electron transfer interaction between donor and acceptor molecules in mixture. The electron transfer rate constant for charge separation ($k_{ET(CS)}$) was calculated to be 4.75 $\times$ 10^9 s^{-1} and 5.0 $\times$ 10^9 s^{-1} for product **1** & **2** respectively using the following eqn (1)

$$k_{ET(CS)} = \frac{1}{\tau(\text{mixture})} - \frac{1}{\tau(\text{P3HT})} \quad (1)$$

where, τ(P3HT) and τ(mixture) are lifetimes of singlet excited states of pure P3HT and in mixture respectively. According to ref. 32, $k_{ET(CS)}$ for P3HT : PCBM in *o*-dichlorobenzene solution is calculated to be 4.6 $\times$ 10^8 s^{-1}, which is one order less than product **1** & **2**. The efficiency of charge separation ($\phi_{(CS)}$) was calculated using following eqn (2)

$$\phi_{(CS)} = \frac{\frac{1}{\tau(\text{mixture})} - \frac{1}{\tau(\text{P3HT})}}{\frac{1}{\tau(\text{mixture})}} \quad (2)$$

Product **2** shows better charge transfer efficiency (85%) than product **1** (81%) calculated from eqn (2). To further understand the charge transfer process between fullerene acceptor on mixing with donor polymer it is important to study the photophysics of excited states involved in charge transfer process forming charge separated states.[36] Charge separated states consist of coulombically bound electron–hole pairs primarily located on HOMO of donor and LUMO of acceptor respectively. Transient absorption studies have been performed to characterize the excited state dynamics in picoseconds time domain in P3HT : methanofullerene blends. In pump-probe measurement 530 nm excitation wavelength was used to selectively excite P3HT. Neat P3HT solution was used as reference for determining charge-transfer mechanism in blends. The transient absorption spectrum of P3HT below 2 ps shows photobleaching due to ground state absorption and emissions (Fig. 9). Transient absorption appears after 50 ps between 750–800 nm which is ascribed to charge separated state of polymer cation and anion undergoing relaxation within 0.5 ns.

The transient absorption spectra of P3HT mixture with product **1** & **2** (equimolar) show similar pattern and representative spectra of product **1** is shown in Fig. 10A using excitation wavelength of 530 nm for P3HT excitation. Similar to neat

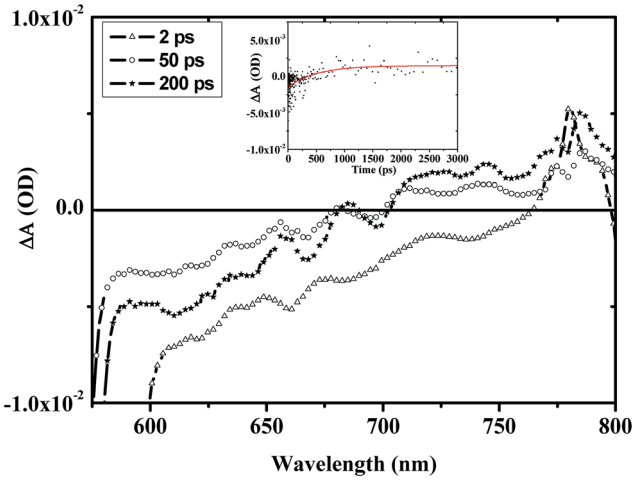

Fig. 9 Transient absorption spectra of neat P3HT solution after 2, 50 and 200 ps. Inset shows decay kinetics at 770 nm and red is the fitting curve.

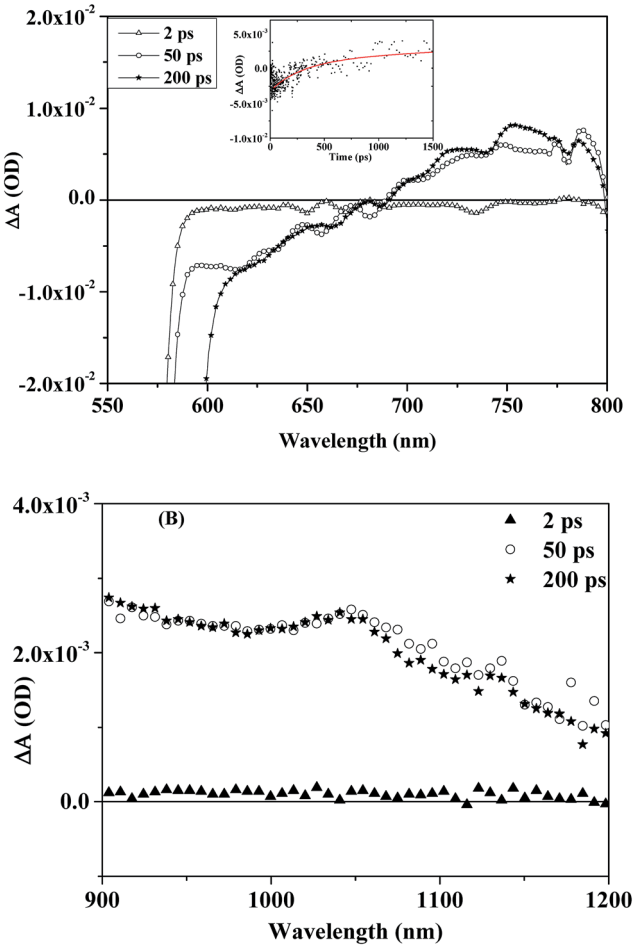

Fig. 10 (A) Transient absorption spectra of P3HT : acceptor mixture solution after 2, 50 and 200 ps for charge transfer species formation. Inset shows decay kinetics at 750 nm, (B) transient absorption spectra of $C_{60}^{-\bullet}$.

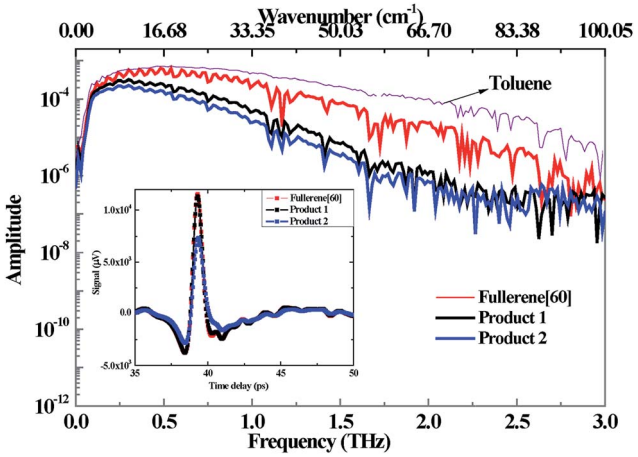

Fig. 11 Terahertz spectra of toluene, fullerene[60], product 1 & 2 (frequency domain profile). Inset shows the terahertz pulse signal (time domain profile) transmitted through the solutions of fullerene[60], product 1 & 2.

P3HT, mixtures also show photo-bleaching at 650, 670 and 690 nm for ground state absorption and emission bleaching at 730 nm. Strong transient absorption appears between 700 and 770 nm after 50 ps for P3HT cation radical formation. Simultaneously, after 50 ps a transient absorption appears at ~1050 nm for fullerene anion radical formation (Fig. 10B).[37]

The decay kinetics of transient species (P3HT cation radical) is best fitted with biexponential fitting with a short lived species of 0.2 ns and long live species of ~2 ns. The short lived component can be best ascribed to be P3HT singlet excited state which undergoes geminate intermolecular charge recombination (corroborating with PL decay kinetics) and long lived component to be charge separated state and product 2 in fact shows much less geminate recombination component (<10%) which may be due to better compatibility with P3HT and presence of electron donating groups in exohedral chain.

Materials have also been characterized by terahertz spectroscopy and further used for calculation of photoconductivity in terahertz range. Development of terahertz technology has now made it feasible to understand the charge carrier behaviour in variety of carbon materials.[38–40] Terahertz (THz) spectroscopy covers the far infrared part of the electromagnetic radiation and in the present work, study has been performed in the range of 0–3 THz corresponding to 0–12.4 meV in equimolar concentration of products and parent fullerene in toluene solution (Fig. 11).[41] The reference toluene shows clear window from 0–2.17 THz and a few peaks up to 3 THz.

Terahertz radiations are sensitive to the vibrational states of the compound. As can be seen in Fig. 11, product **1** & **2** both show completely different spectral profile compared to parent fullerene (C_{60}) where more intense absorption peaks can be seen in between 1.5–2.5 THz in the products (Table 1) however, a relationship between peaks and molecular structure is still to be established. There are several modes of vibration of fullerene compounds which are unidentified by other spectroscopic techniques (like FTIR, Raman *etc.*) but can be probed by THz. We observed increased intensity peaks at 1.108, 1.668, 1.920 and 2.26 THz while a new strong peak appears at 2.037 THz in products compared to parent fullerene. This can be attributed to new bond formation over fullerene ball and change of 60π electron system to 58π electron system. Inset of Fig. 11 shows the terahertz time pulse signal where, product **1** shows equal amplitude to the fullerene and ~36% intensity reduction in product **2**. Table 1 shows the terahertz spectral finger print spectra for fullerene[60], product **1** & **2**.

Lastly we studied the photoconductivity (σ) of product **1** & **2** and compared with fullerene[60] in toluene solution by time domain terahertz spectroscopy using following eqn (3)[42,43]

$$\Delta\sigma = \frac{1+n}{Z_o d}\left(\frac{1}{1+\Delta T/T} - 1\right) \quad (3)$$

where, n is the refractive index of the solution (=1.496 for toluene); Z_o is impedance of free space (=377 Ω) and $\Delta T/T$ is change in transmittance.

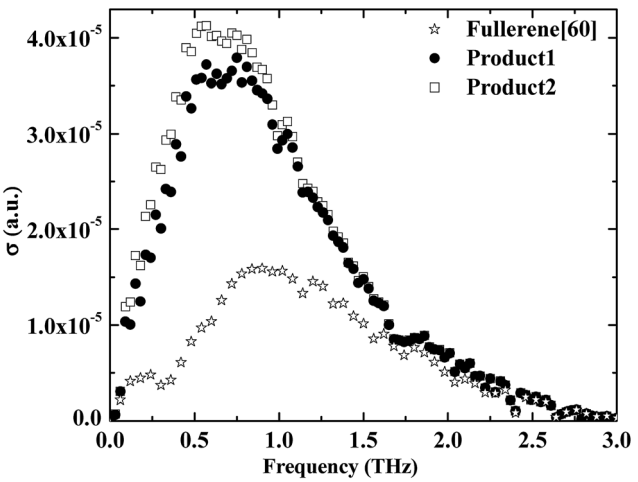

Fig. 12 Photoconductivity plot of fullerene[60], product 1 and 2 in toluene solution by terahertz spectroscopy.

Table 1 Terahertz spectral peaks of reference toluene, fullerene[60], product 1 & 2

Reference toluene	Fullerene[60]	Product **1**	Product **2**
2.17, 2.2, 2.26, 2.37, 2.4, 2.47, 2.65, 2.8, 2.89, 2.98	1.108, 1.179, 1.219, 1.425, 1.605, 1.666, 1.877, 2.173, 2.208, 2.235, 2.281, 2.474, 2.640, 2.671, 2.810, 2.833, 2.871	0.551, 0.747, 1.108, 1.169, 1.214, 1.415, 1.605, 1.371, 1.877, 1.922, 2.038, 2.038, 2.084, 2.169, 2.223, 2.339, 2.385, 2.454, 2.508, 2.539, 2.624, 2.693, 2.786	0.551, 0.742, 1.108, 1.175, 1.222, 1.414, 1.599, 1.661, 1.877, 1.916, 2.039, 2.263, 2.348, 2.402, 2.448, 2.548, 2.671, 2.749, 2.795, 2.549

It can be clearly seen in Fig. 12, photoconductivity is enhanced on increasing incident frequency and both products **1** & **2** show highest photoconductivity between 0.5–1 THz in contrast to PC61BM which is reported to show negligible photoconductivity in terahertz region.[44,45] Huge enhancement in conductivity is observed on conversion of parent fullerene to product **1** & **2**. Product **2** further shows better photoconductivity than product **1** indicating enhanced generation of mobile charge carrier on photoexcitation.

3. Conclusions

In conclusion we have synthesized new methanofullerene derivatives with different exohedral groups for their charge transfer studies in blend with P3HT donor polymer. The importance of the work lies in the methodology for 1,3 dipolar cycloaddition reaction of fullerene which is very eco-friendly as the hazardous materials are totally avoided and the photophysical properties of these materials as acceptor with P3HT donor polymer. The structure of the products has been completely characterized by spectroscopic techniques including terahertz spectroscopy. Transient fluorescence and absorption spectroscopy clearly shows the efficient charge separation and formation of long lived charge separated states in both the products with high photoconductivities making them potential candidates for organic electronics.

4. Experimental section

4.1 Materials and characterization

All chemicals and reagents were purchased from Sigma-Aldrich and used without further purification. Solvents were purified by distillation before use. Poly(3-hexyl)thiophene was also purchased from Sigma-Aldrich. All the products were characterized by Fourier transform infrared spectroscopy (FTIR) using KBr pallets on Perkin Elmer FTIR Spectrum 2. FTIR spectra were collected over a range from 3500 to 500 cm^{-1}. A background in air was done before scanning the samples. For terahertz time domain spectroscopy, two identical < 110 > cut ZnTe crystals of thickness 0.2 mm were used for THz radiation generation and detection. Ultra short pulses of duration 50 fs, wavelength 800 nm at the repetition rate 1 kHz coming out of a Kerr-lens mode locked Ti:Sapphire laser amplifier (Coherent Libra) were used. By optical rectification method single cycle THz pulse has been generated and detected by electro-optic sampling. A mechanical chopper has been used to increase signal to noise ratio. The generated THz radiation first collimated and then focused by two parabolic mirrors. The focus position of the THz is the position where the sample under investigation is to be placed for spectroscopy. After focusing, the THz beam is again collimated and focused on the detection crystal by another two parabolic mirrors. A motorized delay stage was used to introduce delay between the THz pulse and the optical probe pulse. UV-vis spectroscopy measurement was performed on a Shimadzu UV-vis spectrophotometer (UV-1800) using 1 mg/3 mL solution in chloroform. ^{1}H and ^{13}C NMR spectra were recorded on Jeol 400 MHz spectrometer in $CDCl_3$ using tetramethylsilane as internal standard. Molecular weights of the products were confirmed from MALDI-TOF-TOF mass spectrometry on AB SCIEX using α-cyano 4-hydroxy cinnamic acid matrix. Thermal gravimetric analysis (TGA) was run under nitrogen flow of 20 mL min^{-1} using Perkin Elmer (Pyris 1) TGA instrument and mass loss was recorded as a function of temperature. The samples were heated from room temperature to 950 °C at a ramp rate of 10 °C min^{-1}. Cyclic voltammetry measurements were performed using a three electrode standard configuration with a platinum wire as counter electrode and Ag wire as reference electrode and Pt-disc as working electrode in a 0.1 M $TBAPF_6$ (tetra-*n*-butylammoniumhexafluorophosphate) in *o*-dichlorobenzene solution as electrolyte at 20 mV s^{-1} scan rate. Current *vs.* voltage was measured on an Autolab potentiostat. Emission fluorescence measurements were performed on Varian (CARY eclipse) Fluorescence Spectrophotometer in chloroform solution using 530 nm excitation wavelength. Horiba JobinYvon (Fluorohub) time correlated single photon counting system (TCSPC) was used to record time resolved fluorescence. To perform ultrafast optical pump-probe spectroscopy a train of optical pulse from a Ti:Sapphire laser amplifier (35 fs, 4 mJ per pulse, 1 kHz, 800 nm) was splitted into two beams with a beam splitter. One with high intensity was used as a pump and an optical parametric amplifier (TOPAS, Light Conversion) was employed to vary the wavelength of this pump beam from 190 nm to 2600 nm. The other beam with weak intensity was propagated through a CaF_2 crystal to generate white light continuum (WLC) covering the whole spectrum of visible light to be used as a probe beam. The probe beam was optically delayed with respect to pump beam using a computer-controlled delay stage. The intrinsic temporal resolution of delay stage is 7 fs. Here we have performed ultrafast pump-probe spectroscopy using 530 nm as a pump beam at normal incidence and the changes in absorption was detected by using a gated CMOS detector. The time resolved study was performed using HELIOS (Ultrafast systems) spectrometer.

4.2 Synthesis

4.2.1. General method of synthesis of chalcone (1a). Acetophenone (2 mM, 240 mg) and 2-hydroxy 5-nitro benzaldehyde (2 mM, 334 mg) were dissolved in 100 mL ethanol. To this 40% NaOH solution (10 mL) was added with stirring at room temperature. Progress of reaction was monitored by TLC. Finally reaction mixture was acidified with dilute HCl. Solid was filtered and washed several times with water and dried. Purified by column chromatography using ethyl acetate : *n*-hexane (70 : 30) mixture. Yield: 85%. FTIR (cm^{-1}) 3063, 1656, 1600, 1511, 1481, 1351, 1284, 1098, 919, 718, 623; ^{1}H NMR ($CDCl_3$, 400 MHz) δ (ppm) 6.7 (1H), 7.4 (3H), 7.5 (2H), 7.8 (3H), 8.1 (1H); ^{13}C NMR ($CDCl_3$, 100 MHz) δ (ppm) 118, 119, 128.2, 128.5, 129.7, 131.6, 134, 137, 140, 145, 166, 195; *m*/*z* 269 (M + 1).

4.2.2. General method of synthesis of tosylhydrazone of chalcone or cinnamaldehyde (1b, 2b). To the methanolic solution (25 mL) of chalcone (1 mM, 269 mg) or cinnamaldehyde (1 mM, 178 mg), *p*-toluenesulfonyl hydrazide (1.2 mM, 223 mg) was added and refluxed with stirring for ~6 h followed by

stirring at room temperature over night. Crystals of hydrazone came out of solution on cooling and collected after washing with cold methanol. Yield: ~75%. **1b**: FTIR (cm^{-1}) 3573, 3100, 3067, 1623, 1600, 1511, 1481, 1336, 1165, 1090, 580; ^{1}H NMR ($CDCl_3$, 400 MHz) δ (ppm) 2.36 (3H), 6.9 (1H), 7.2 (1H), 7.3 (2H), 7.6 (4H), 7.7 (2H), 7.78 (1H), 7.9 (1H), 8.1 (2H). **2b**: FTIR (cm^{-1}) 3201, 1628, 1608, 1522, 1295, 1172, 1038, 822, 677; ^{1}H NMR ($CDCl_3$, 400 MHz) δ (ppm) 2.3 (3H), 3.4 (3H) 6.6 (1H), 6.83 (2H), 6.29 (1H), 7.1 (1H), 7.2 (3H), 7.5 (1H), 7.8 (2H); ^{13}C NMR ($CDCl_3$, 100 MHz), δ (ppm) 21.5, 55.8, 108.9, 114, 121, 127, 128, 129, 135, 139, 144, 146, 150.

4.2.3. One pot synthesis of methanofullerene adducts (1 & 2). Hydrazone (0.14 mM) was dissolved in dichloromethane (10 mL) and cooled down to 0 °C. Catalytic amount of triethyl amine was added and stirred for three hours at this temperature. A solution of fullerene[60] (0.3 eq.) in *o*-dichlorobenzene was added and temperature was raised to 75–80 °C. Stirred at this temperature for 18 hours followed by precipitation with methanol. Solid was collected by centrifugation and loaded on column (200 mm × 18 mm) for purification with toluene/hexane or dichloromethane/hexane mixtures. Product **1**, isolated [5,6]fulleroid is further refluxed in *o*-dichlorobenzene for 5 hours to convert into [6,6]methanofullerene.

*Product **1**.* Yield: ~30%; FTIR (ν, cm^{-1}) 3458, 2937, 1634, 1511, 1265, 1180, 811; λ_{max} (nm): 410, 530, 597, 697; ^{1}H NMR ($CDCl_3$, 400 MHz), δ (ppm) 6.9 (d, J = 7.56 Hz, 1H), 7.1 (m, 4H), 7.19 (s, 1H), 7.39 (m, 4H); ^{13}C NMR ($CDCl_3$, 100 MHz), δ (ppm) 64 (C_{61}), 89 ($C(sp^3)$ of C_{60}), 115, 120.5, 122.5, 123, 123.5, 124, 126, 128.5, 128.6, 132, 132.1, 133, 133.4, 133.6, 136, 136.5, 137, 138, 138.5, 139, 139.6, 140, 140.8, 141, 141.5, 142, 143; m/z 972 (M − 1).

*Product **2**.* Yield: ~32%; FTIR (cm^{-1}) 3436, 2923, 1632, 1459, 1384, 1096, 1055, 806; λ_{max} (nm): 408, 432, 697; ^{1}H NMR ($CDCl_3$, 400 MHz), δ (ppm) 3.8 (s, 3H), 4.8 (d, J = 8.0 Hz, 1H), 6.7 (dd, J = 7.6 Hz, 1H), 6.9 (d, J = 8.0 Hz, 1H), 7.1 (m, 2H), 7.19 (s, 1H); ^{13}C NMR ($CDCl_3$, 100 MHz), δ (ppm) 30.5, 67.7 (C_{61}), 86.0 ($C(sp^3)$ of C_{60}), 86.2 ($C(sp^3)$ of C_{60}), 115, 124.3, 124.5, 125, 125.5, 125.7, 126.5, 127, 128.5, 128.8, 129, 130, 131, 131.5, 132; m/z 882 (M + 1).

Acknowledgements

The authors acknowledge CSIR TAPSUN program for funding this research work. One of the authors, SN is thankful to TAPSUN project for her fellowship.

References

1 E. E. Maroto, M. Izquierdo, S. Reboredo, J. Marco-Martínez, S. Filippone and N. Martín, *Acc. Chem. Res.*, 2014, **47**, 2660–2670.
2 M. Prato, *J. Mater. Chem.*, 1997, **7**, 1097–1109.
3 M. T. Dang, L. Hirsch, G. Wantz and J. D. Wuest, *Chem. Rev.*, 2013, **113**, 3734–3765.
4 P. Hudhomme, *EPJ Photovoltaics*, 2013, **4**, 40401.
5 E. Nakamura and H. Isobe, *Acc. Chem. Res.*, 2003, **36**, 807–815.
6 S. Bosi, T. Da Ros, G. Spalluto and M. Prato, *Eur. J. Med. Chem.*, 2003, **38**, 913–923.
7 E. E. Maroto, S. Filippone, M. Suárez, R. Martínez-Álvarez, A. de Cózar, F. P. Cossío and N. Martín, *J. Am. Chem. Soc.*, 2014, **136**, 705–712.
8 W. Sliwa, *Fullerene Sci. Technol.*, 1995, **3**, 243–281.
9 A. A. Peyghn and M. Noei, *Chem. Pap.*, 2014, **68**, 409–416.
10 H. T. Yang, W. L. Ren, C. B. Miao, C. P. Dong, Y. Yang, H. T. Xi, Q. Meng, Y. Jiang and X. Q. Sun, *J. Org. Chem.*, 2013, **78**, 1163–1170.
11 F. H. Wu, X. D. Yu, S. H. Wu, H. M. Wu, J. F. Xub and X. F. Lao, *J. Fluorine Chem.*, 1998, **90**, 57–58.
12 M. D. Tzirakis and M. Orfanopoulos, *Chem. Rev.*, 2013, **113**, 5262–5321.
13 Y. He and Y. Li, *Phys. Chem. Chem. Phys.*, 2011, **13**, 1970–1983.
14 J. C. Hummelen, B. W. Knight, F. LegPeq, F. Wudl, J. Yao and C. L. Wilkins, *J. Org. Chem.*, 1995, **60**, 532–538.
15 M. Yamada, T. Akasaka and S. Nagase, *Chem. Rev.*, 2013, **13**, 7209–7264.
16 R. Kumar, S. Naqvi, N. Gupta and S. Chand, *RSC Adv.*, 2014, **4**, 15675–15677.
17 Y. Y. Lai, Y. J. Cheng and C. S. Hsu, *Energy Environ. Sci.*, 2014, **7**, 1866–1883.
18 F. G. Brunetti, R. Kumar and F. Wudl, *J. Mater. Chem.*, 2010, **20**, 2934–2948.
19 S. C. Chuanga, C. W. Chiua, S. C. Chienb, C. W. Chuc and F. C. Chen, *Synth. Met.*, 2011, **161**, 1264–1269.
20 F. B. Kooistra, J. Knol, F. Kastenberg, L. M. Popescu, W. J. H. Verhees, J. M. Kroon and J. C. Hummelen, *Org. Lett.*, 2007, **9**, 551–554.
21 A. R. Tuktarov, V. V. Korolev and U. M. Dzhemilev, *Russ. J. Org. Chem.*, 2010, **46**, 588–589.
22 A. I. McIntosh, B. Yang, S. M. Goldup, M. Watkinson and R. S. Donnan, *Chem. Soc. Rev.*, 2012, **41**, 2072–2082.
23 J. G. Muller, J. M. Lupton, J. Feldmann, U. Lemmer, M. C. Scharber, N. S. Sariciftci, C. J. Brabec and U. Scherf, *Phys. Rev. B: Condens. Matter Mater. Phys.*, 2005, **72**, 195208.
24 P. E. Keivanidis, T. M. Clarke, S. Lilliu, T. Agostinelli, J. E. Macdonald, J. Durrant, D. D. C. Bradley and J. Nelson, *J. Phys. Chem. Lett.*, 2010, **1**, 734–738.
25 H. Ohkita, S. Cook, Y. Astuti, W. Duffy, S. Tierney, W. Zhang, M. Heeney, I. McCulloch, J. Nelson, D. D. C. Bradley and J. R. Durrant, *J. Am. Chem. Soc.*, 2008, **130**, 3030–3042.
26 A. La Rosa, K. Gillemot, E. Leary, C. Evangeli, M. T. González, S. Filippone, G. Rubio-Bollinger, N. Agraït, C. J. Lambert and N. Martín, *J. Org. Chem.*, 2014, **79**, 4871–4877.
27 H. U. Kim, D. Mi, J. H. Kim, J. B. Park, S. C. Yoon, U. C. Yoon and D. H. Hwang, *Sol. Energy Mater. Sol. Cells*, 2012, **105**, 6–14.
28 R. Arnz, J. W. D. M. Carneiro, W. Klug, H. Schmickler, E. Vogel, R. Breuckmann and F. G. Klaerner, *Angew. Chem., Int. Ed. Engl.*, 1991, **30**, 683–686.
29 G.-W. Wang, Y.-W. Dong, P. Wu, T.-T. Yuan and Y.-B. Shen, *J. Org. Chem.*, 2008, **73**, 7088–7095.
30 G. W. Wang, Y. J. Li, R. F. Peng, Z. H. Liang and Y. C. Liu, *Tetrahedron*, 2004, **60**, 3921–3925.

31 J. L. Bredas, R. Silbey, D. S. Boudreaux and R. R. Chance, *J. Am. Chem. Soc.*, 1983, **105**, 6555–6559.
32 K. Gmucova, V. Nadazdy, F. Schauer, M. Kaiser and E. Majkova, *J. Phys. Chem. C*, 2015, **119**, 15926–15934.
33 M. Reyes-Reyes, K. Kim, J. Dewald, R. López-Sandoval, A. Avadhanula, S. Curran and D. L. Carroll, *Org. Lett.*, 2005, **7**, 5749–5752.
34 D. Jarzab, F. Cordella, M. Lenes, F. B. Kooistra, P. W. H. Blom, J. C. Hummelen and M. A. Loi, *J. Phys. Chem. B*, 2009, **113**, 16513–16517.
35 J. Piris, T. E. Dykstra, A. A. Bakulin, P. H. M. van Loosdrecht, W. Knulst, M. T. Trinh, J. M. Schins and L. D. A. Siebbeles, *J. Phys. Chem. C*, 2009, **113**, 14500–14506.
36 G. Grancini, D. Polli, D. Fazzi, J. Cabanillas-Gonzalez, G. Cerullo and G. Lanzani, *J. Phys. Chem. Lett.*, 2011, **2**, 1099–1105.
37 D. M. Guldi and M. Prato, *Acc. Chem. Res.*, 2000, **33**, 695–703.
38 T. I. Jeon, J. H. Son, K. H. An, Y. H. Lee and Y. S. Lee, *J. Appl. Phys.*, 2005, **98**, 034316.
39 M. Takahashi, *Crystals*, 2014, **4**, 74–103.
40 X. Ai, M. C. Beard, K. P. Knutsen, S. E. Shaheen, G. Rumbles and R. J. Ellingson, *J. Phys. Chem. B*, 2006, **110**, 25462–25471.
41 A. Rahman, *J. Mol. Struct.*, 2011, **1006**, 59–65.
42 P. Parkinson, J. L-Hughes, M. B. Johnston and L. M. Herz, *Phys. Rev. B: Condens. Matter Mater. Phys.*, 2008, **78**, 115321.
43 K. P. H. Lui and F. A. Hegmann, *Appl. Phys. Lett.*, 2001, **78**, 3478–3480.
44 Z. Jin, D. Gehrig, C. D. Smith, E. J. Heilweil, F. Laquai, M. Bonn and D. Turchinovich, *J. Phys. Chem. Lett.*, 2014, **5**, 3662–3668.
45 P. D. Cunningham and L. M. Hayden, *J. Phys. Chem. C*, 2008, **112**, 7928–7935.